JACS
JOURNAL OF THE AMERICAN CHEMICAL SOCIETY
Article
pubs.acs.org/JACS

# An Fe-$N_2$ Complex That Generates Hydrazine and Ammonia via Fe=$NNH_2$: Demonstrating a Hybrid Distal-to-Alternating Pathway for $N_2$ Reduction

Jonathan Rittle and Jonas C. Peters*

Division of Chemistry and Chemical Engineering, California Institute of Technology (Caltech), Pasadena, California 91125, United States

Supporting Information

**ABSTRACT:** Biological $N_2$ fixation to $NH_3$ may proceed at one or more Fe sites in the active-site cofactors of nitrogenases. Modeling individual $e^-/H^+$ transfer steps of iron-ligated $N_2$ in well-defined synthetic systems is hence of much interest but remains a significant challenge. While iron complexes have been recently discovered that catalyze the formation of $NH_3$ from $N_2$, mechanistic details remain uncertain. Herein, we report the synthesis and isolation of a diamagnetic, 5-coordinate Fe=$NNH_2^+$ species supported by a tris(phosphino)silyl ligand via the direct protonation of a terminally bound Fe-$N_2^-$ complex. The Fe=$NNH_2^+$ complex is redox-active, and low-temperature spectroscopic data and DFT calculations evidence an accumulation of significant radical character on the hydrazido ligand upon one-electron reduction to $S = {}^1/_2$ Fe=$NNH_2$. At warmer temperatures, Fe=$NNH_2$ rapidly converts to an iron hydrazine complex, Fe-$NH_2NH_2^+$, via the additional transfer of proton and electron equivalents in solution. Fe-$NH_2NH_2^+$ can liberate $NH_3$, and the sequence of reactions described here hence demonstrates that an iron site can shuttle from a distal intermediate (Fe=$NNH_2^+$) to an alternating intermediate (Fe-$NH_2NH_2^+$) en route to $NH_3$ liberation from $N_2$. It is interesting to consider the possibility that similar hybrid distal/alternating crossover mechanisms for $N_2$ reduction may be operative in biological $N_2$ fixation.

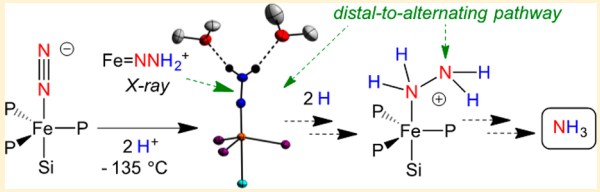


## INTRODUCTION

The proton-coupled reduction of nitrogen ($N_2$) to ammonia ($NH_3$) by nitrogenase enzymes sustains life and has been under study for decades. Known nitrogenases employ a cofactor comprised of seven Fe-atoms and one additional metal site (Mo, V, or Fe).[1] Despite a suite of crystallographic, theoretical, and spectroscopic studies,[2] the mechanistic details of $N_2$ reduction and the metallic site(s) of $N_2$ coordination are uncertain.

The feasibility of $N_2$ reduction at an Fe or Mo site has been tested with synthetic model complexes.[3] Well-defined Mo systems have been reported to catalyze the direct reduction of $N_2$ to $NH_3$ in the presence of proton and electron equivalents,[4] and our laboratory has recently disclosed Fe complexes that furnish catalytic yields of $NH_3$ from $N_2$.[5] While synthetic studies of the Mo systems have revealed a number of isolable Mo($N_xH_y$) species that inform likely mechanistic scenarios of $N_2$ activation and overall reduction,[6,4c] similar studies on the Fe catalyzed systems are challenged by the high reactivity of some of the putative Fe($N_xH_y$) intermediates and their varied spin states.

An iron hydrazido(2−) complex, Fe=$NNH_2^+$, has been invoked as a likely intermediate in Fe-catalyzed reaction mixtures with a tris(phosphine)borane (TPB) iron system (TPB = tris(2-(diisopropylphosphino)phenyl)borane)).[5,7] Its detection *in operando* when *both* strong acid and reductant are present is not feasible; the species is far too reactive under such conditions. We therefore generated {[TPB]Fe=$NNH_2$}$^+$ at low temperature by double protonation of {[TPB]Fe($N_2$)}$^-$ in the absence of exogenous reductant and characterized this species with a suite of spectroscopic techniques including EPR/ENDOR, XAS, and Mössbauer spectroscopies.[7] {[TPB]Fe=$NNH_2$}$^+$ decays rapidly at temperatures above −78 °C, frustrating our attempts to purify and study it by X-ray crystallography and to map its further reactivity patterns.

The complex {[$SiP^{iPr}_3$]Fe($N_2$)}$^-$ ([$SiP^{iPr}_3$] = tris(2-(diisopropylphosphino)phenyl)silyl$^{(-)}$) is isostructural to the {[TPB]Fe($N_2$)}$^-$ catalyst. While catalytic amounts of $NH_3$ (7.0(1) equiv of $NH_3$ per Fe) are generated when {[TPB]Fe($N_2$)}$^-$ is exposed to the originally reported catalytic conditions (−78 °C in $Et_2O$, 1 atm $N_2$, 48 equiv of {$H(OEt_2)_2$}{$BAr^F{}_{24}$}, 58 equiv of $KC_8$), {[$SiP^{iPr}_3$]Fe($N_2$)}$^-$ liberates substoichiometric amounts of $NH_3$ (0.8(1) equiv of $NH_3$ per Fe) under the same conditions.[5] We surmised that the doubly protonated form of this species, {[$SiP^{iPr}_3$]Fe=$NNH_2$}$^+$, might be more readily characterized than {[TPB]Fe=$NNH_2$}$^+$ owing to its predicted closed-shell configuration (18-electron species). Herein, we report its synthesis and high-resolution crystal structure. This isolable Fe=$NNH_2^+$ species is derived from protonation of its Fe($N_2$)$^-$ congener. We additionally explore the redox pairs Fe=$NNH_2^+$/Fe=$NNH_2$ and the methyl analogues Fe=$NNMe_2^+$/Fe=$NNMe_2$ and demonstrate the overall conversion

**Received:** February 2, 2016
**Published:** March 3, 2016





DOI: 10.1021/jacs.6b01230
J. Am. Chem. Soc. 2016, 138, 4243−4248

of $Fe{=}NNH_2^+$ to $NH_3$ via an $Fe\text{-}NH_2NH_2^+$ intermediate. These observations in sum establish that an iron model system can traverse both distal ($Fe{=}NNH_2$) and alternating ($Fe\text{-}NH_2NH_2$) intermediates en route to $NH_3$ formation from $N_2$, providing synthetic precedent for a new hybrid distal-to-alternating crossover pathway for Fe-mediated $N_2$ reduction (Scheme 1).[7,8]

**Scheme 1. Distal and Alternating Pathways for $N_2$ Reduction, and the Hybrid Crossover Pathway Emphasized Herein**

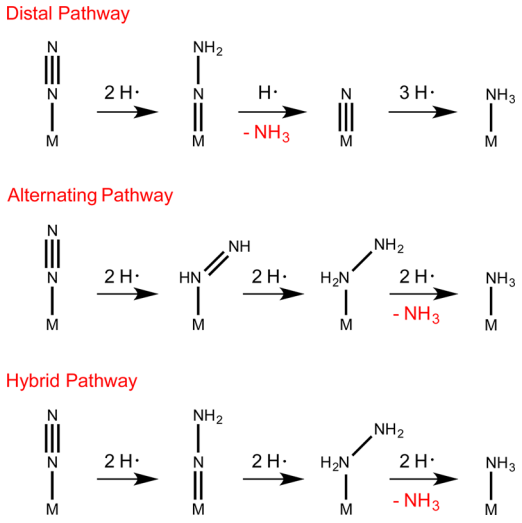


## RESULTS AND DISCUSSION

As for $\{[TPB]Fe(N_2)\}^-$,[7] the successful protonation of $Fe(N_2)$ complexes supported by the $[SiP^{iPr}_3]$ ligand required very low temperatures.[9] For example, the addition of 1 or 2 equiv of the acid $\{H(OEt_2)_2\}\{BAr^F_{24}\}$ to $\{K(Et_2O)\}\{[SiP^{iPr}_3]Fe(N_2)\}$ (**1**) at −78 °C resulted in the immediate formation of mixtures containing both one-electron oxidized $[SiP^{iPr}_3]Fe(N_2)$ (**2**) and two-electron oxidized $\{[SiP^{iPr}_3]Fe(N_2)\}\{BAr^F_{24}\}$ (**3**).[9] These proton-induced oxidation reactions likely proceed via an unstable and as yet unobserved iron diazenido species, $[SiP^{iPr}_3]Fe(NNH)$ (**4**), structurally and electronically related to the previously reported and stable silyldiazenido complex, $[SiP^{iPr}_3]Fe(NNSiMe_3)$.[9a] An alternative hydride product, $[SiP^{iPr}_3]Fe(N_2)(H)$, that would derive from protonation at iron instead of $N_2$ is not observed; $[SiP^{iPr}_3]Fe(N_2)(H)$ is a very

**Scheme 2. Functionalization of $[SiP^{iPr}_3]Fe(N_2)$ Complexes**

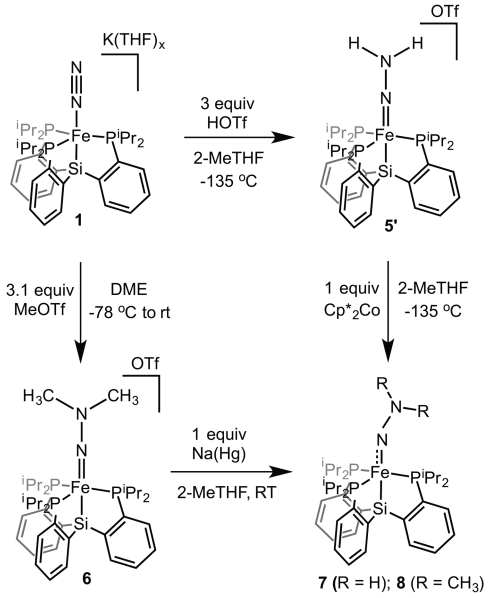


stable complex that has been characterized,[10] and were it produced as the kinetic product of protonation, we would anticipate observing it as it should also be the thermodynamically preferred isomer.

Combination of **1** with 5 equiv of $\{H(OEt_2)_2\}\{BAr^F_{24}\}$ in thawing 2-MeTHF at −135 °C instead produced a pale lavender solution (Figure 1A) with UV−visible features that are distinct from the oxidation products $Fe\text{-}N_2$ **2** and $Fe\text{-}N_2^+$ **3**. The *in situ* $^{57}$Fe Mössbauer spectrum (Figure 1B) collected on similarly prepared solutions derived from $^{57}$Fe-enriched **1** evidences a new integer-spin Fe complex ($\delta$ = 0.126 mm/s and $\Delta E_Q$ = 1.484 mm/s) assigned as $Fe{=}NNH_2^+$ **5** (*vide infra*), that constitutes ∼90% of the Fe in solution; $Fe\text{-}N_2^+$ **3** is present as a minor (∼10%) component. Compound **5** is persistent for hours in solution at temperatures of −78 °C once prepared in this manner but is increasingly unstable as the solution is warmed further.

The isolation of **5** as a crystalline solid free of Fe-containing impurities was facilitated by substitution of the $BAr^F_{24}$ counteranion with a less-soluble analogue. The reaction of **1** with 3 equiv of trifluoromethanesulfonic acid (HOTf) proceeded similarly at −135 °C, but this compound (**5′**)

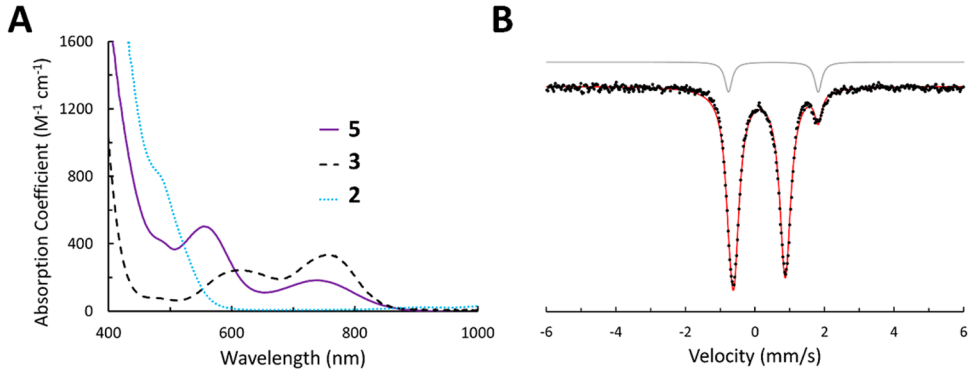


**Figure 1.** Spectroscopic data collected *in situ* on compound **5**. (A) UV−visible absorbance spectra of **3**, **2**, and **5**. Spectra were collected in 2-MeTHF at −80 °C. (B) Zero-field $^{57}$Fe Mössbauer spectra of $^{57}$Fe-enriched **5** as a 3 mM solution in 2-MeTHF prepared from **1** and collected at 80 K. The minor component (10%) was identified as complex **3** derived from competitive oxidation.



DOI: 10.1021/jacs.6b01230
J. Am. Chem. Soc. 2016, 138, 4243−4248

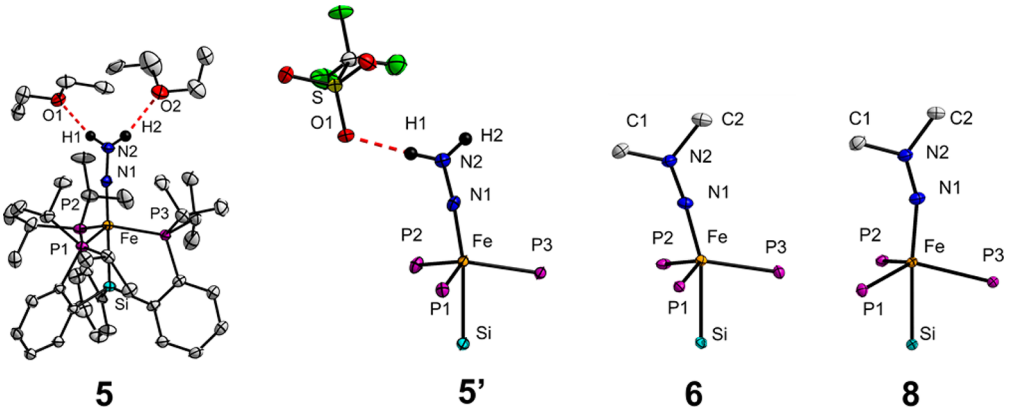


**Figure 2.** X-ray diffraction crystal structure of **5** and core-atom structures of **5′**, **6**, and **8** with thermal ellipsoids drawn at 50% probability. Hydrogen atoms (excep for the N–H's), the $BAr^{F}_{24}$ counteranion of **5**, the triflate counteranion of **6**, and co-crystallized solvent molecules have been removed for clarity. Refer to the Supporting Information for complete crystallographic details.

**Table 1. Crystallographic Bond Metrics**

| | 5 | 5′ | 6 | 8 |
|---|---|---|---|---|
| Fe–N[a] | 1.672(2) | 1.668(2) | 1.691(2) | 1.773(1) |
| N–N[a] | 1.272(3) | 1.273(3) | 1.270(3) | 1.276(2) |
| Fe–N–N[b] | 175.3(2) | 175.0(2) | 174.7(2) | 158.63(9) |
| Si–Fe–N[b] | 173.99(6) | 170.82(7) | 164.64(9) | 174.19(4) |

[a]Bond distances in Å. [b]Bond angle in degrees.

could be effectively precipitated out of solution in 49% yield by the addition of pentane at temperatures of −78 °C or lower (Scheme 2). The $^{57}$Fe Mössbauer spectrum of solid **5′** (Supporting Information) reveals a single Fe-containing species with parameters that are similar to those of **5** in frozen solution (Figure 1B). Solid **5′** displays intense vibrational features at 3207 and 3039 cm$^{-1}$ that shift to 2380 and 2241 cm$^{-1}$ in **5′-$d_2$** (prepared from the reaction of **1** with DOTf) assigned to N–H stretching frequencies with strong hydrogen bonding interactions.[11,12] These vibrational features persist in solid samples of **5′** that have been stored for days at −30 °C in the absence of air and moisture.

**Characterization of {[SiP$^{iPr}_3$]Fe═NNH$_2$}$^+$.** The stability of **5** and **5′** in solution at −78 °C permitted growth of single crystals suitable for X-ray diffraction, and their respective structures are depicted in Figure 2. The structures differ in that **5** features an independent $Et_2O$ molecule hydrogen bonded to each of the protons of the $NNH_2$ ligand, and in **5′** the $NNH_2$ protons feature tight hydrogen bonding interactions with the triflate anion, and these interactions form the basis of dimeric $(\mathbf{5'})_2$ units in the crystal lattice (Supporting Information). The structures are nonetheless highly similar with respect to the Fe═$NNH_2^+$ subunit; short Fe–N distances (∼1.67 Å) are found that reflect substantial Fe–N multiple bond character (Table 1), a characteristic feature of most terminal metal hydrazido(2−) complexes.[6,11] The $^{\alpha}$N-atoms display linear geometries, and the location of the nitrogen-bound protons in the Fourier difference map shows trigonal-planar $^{\beta}$N-atoms. The N–N distances (∼1.27 Å) are markedly increased from that

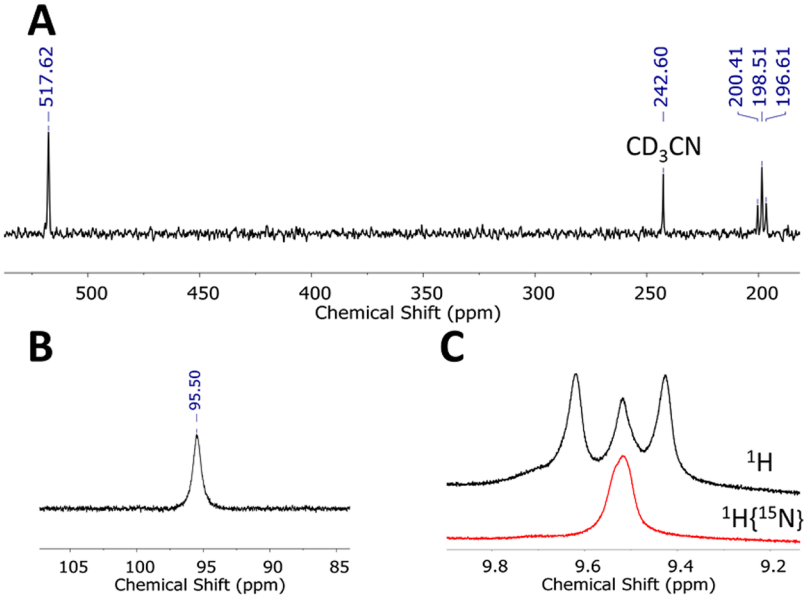


**Figure 3.** NMR spectra of **5′** recorded at −60 °C in 9:1 THF-$d_8$:$CD_3CN$. (A) $^{15}$N NMR spectrum of $^{15}$**N-5′**. (B) $^{31}$P{$^1$H} NMR spectrum of **5′**. (C) Overlaid $^1$H and $^1$H{$^{15}$N} NMR spectra of $^{15}$**N-5′**. The central feature in the $^1$H NMR spectrum results from contamination of $^{15}$**N-5′** with the natural abundance **5′**.



DOI: 10.1021/jacs.6b01230
J. Am. Chem. Soc. 2016, 138, 4243−4248

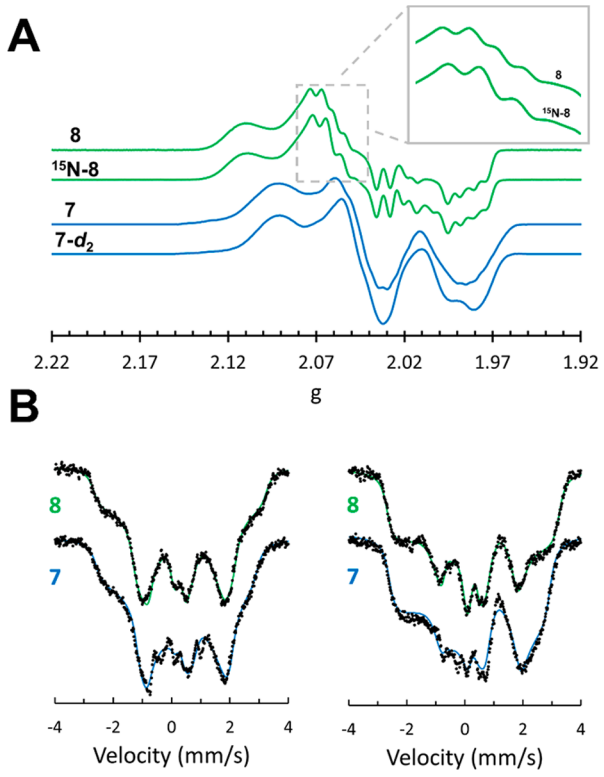


**Figure 4.** (A) X-band EPR spectra of $Fe{=}NNH_2$ **7** and **7-*d*$_2$**, derived from the *in situ* reduction of **5′** or **5′-*d*$_2$**, respectively, with $Cp^*_2Co$ (blue); $Fe{=}NNMe_2$ **8** and **$^{15}$N-8** (green) collected at 77 K in 2-MeTHF glasses. Signals derived from $S = {}^1/_2$ Fe-$N_2$ **2** have been subtracted from the displayed spectra of **7** and **7-*d*$_2$** for clarity. (Inset) Prominent features of **8** that differ in **$^{15}$N-8**. These features arise from hyperfine coupling to single $^{31}$P and single $^{14/15}$N nuclei of comparable magnitude. (B) $^{57}$Fe Mössbauer spectra of *in situ*-prepared **7** and **8** obtained by subtracting out quadrupole doublet impurities from the raw data. A 50 mT magnetic field was applied (left) perpendicular and (right) parallel to the propagation of $\gamma$-beam. The solid lines are theoretical fits to an $S = {}^1/_2$ spin Hamiltonian operating in the slow relaxation regime. Refer to the Supporting Information for a detailed discussion and the derived spin Hamiltonian parameters.

displayed by $\{Na(12\text{-crown-}4)_2\}\{[SiP^{iPr}_3]Fe(N_2)\}$ (1.132(4) Å) and **1** (1.146(4) Å) (Supporting Information).[9a] The N–N distance in **5′** correlates with a broad feature centered at 1443 $cm^{-1}$ in the IR spectrum that shifts to 1401 $cm^{-1}$ in **$^{15}$N-5′** and is assigned to the $\nu$(NN) stretching frequency. IR features of similar energy have been observed in Mo- and $W{=}NNH_2$ complexes.[11] While a number of X-ray diffraction studies on mononuclear[13] and dinuclear[14] Fe complexes that support the isomeric diazene ligand (HN=NH) have been disclosed, **5** and **5′** are the first crystallographically characterized complexes that contain a terminal $Fe{=}NNH_2$ unit. The structural parameters they reveal are consistent with those recently deduced from XAS and ENDOR spectroscopies for the catalytically relevant species, $[TPB]Fe{=}NNH_2^+$.[7]

Although $Fe{=}NNH_2^+$ **5′** is a stable solid, solutions of **5′** decompose at temperatures of 0 °C and higher to an intractable mixture of Fe-containing species. Seeking to prepare a more stable analogue of **5′**, we reacted **1** with excess MeOTf at −78 °C which, upon warming the reaction mixture to room temperature, precipitated $\{[SiP^{iPr}_3]Fe(NNMe_2)\}\{OTf\}$ (**6**) as a purple solid. Unlike the isoelectronic $Fe{=}NNH_2^+$ species, $Fe{=}NNMe_2^+$ **6** is quite stable both in the solid state and in solution. The relevant metrical data derived from the solid-state crystal structure of **6** (Figure 2) are similar to those of **5′** (Table 1).

Compounds **5′** and **6** exhibit diamagnetic ground states, permitting their further characterization by multinuclear NMR spectroscopies (Figure 3A,B,C).[15] A single broad resonance is found in the $^{31}P\{^1H\}$ NMR spectrum of **5′** (Figure 3B), consistent with averaged 3-fold symmetry in solution. Compound **$^{15}$N-5′** exhibits two resonances in the $^{15}$N NMR spectrum at $\delta$ = 518 and 198 ppm, corresponding to the $^{\alpha}$N- and $^{\beta}$N-atoms, respectively (Figure 3A).[6b,16] The resonance at $\delta$ = 198 ppm appears as a triplet of doublets ($^1J_{NH}$ = 96 Hz, $^1J_{NN}$ = 11 Hz) whereas the feature at 518 ppm is broadened due to unresolved coupling to the phosphine ligands. In the $^1$H NMR spectrum (Figure 3C), **$^{15}$N-5′** displays a broad doublet ($^1J_{NH}$ = 97 Hz) at $\delta$ = 9.5 ppm assigned to the $NNH_2$ protons. The magnitude of the $^1J_{NH}$ coupling constant in **5′** is consistent with $sp^2$ hybridization at the $^{\beta}$N-atom[17] and similar to that found in other terminal metal-hydrazido(2−) complexes.[6b,16] These data confirm that the structure of **5′** found in the solid state is maintained in solution. Related NMR data for **6** are provided in the Supporting Information.

**Redox Chemistry of $[SiP^{iPr}_3]Fe{=}NNR_2^+$.** The intermediacy of $Fe{=}NNH_2^+$ **5′** in the formation of $NH_3$ requires additional proton or electron equivalents. Both **5** and **5′** were found to be stable at −78 °C to the presence of additional proton equivalents; we therefore explored the one-electron reduction chemistry of **5′** and $Fe{=}NNMe_2^+$ **6** to generate neutral $[SiP^{iPr}_3]Fe{=}NNH_2$ (**7**) and its methylated derivative $[SiP^{iPr}_3]Fe{=}NNMe_2$ (**8**), respectively. Cyclic voltammetry measurements on THF electrolytes of $Fe{=}NNMe_2^+$ **6** reveal a reversible reduction event at −1.73 V (Supporting Information). The chemical reduction of **6** with 1 equiv of Na(Hg) (Scheme 2) and subsequent workup furnished paramagnetic **8**, whose crystal structure (Figure 2) shows a lengthened Fe–N distance (from 1.69 to 1.77 Å) concomitant with substantial bending at the $^{\alpha}$N-atom from 175° to 159° (Table 1). The $^{\beta}$N-atom retains $sp^2$ hybridization, and the N–N bond length is essentially unchanged. The X-band EPR spectrum of **8** indicates an $S = {}^1/_2$ ground state (Figure 4A, $g_{avg}$ = 2.04), consistent with its room temperature magnetic moment in $C_6D_6$ ($\mu_{eff} = 1.7\mu_B$). Magnetically perturbed $^{57}$Fe Mössbauer studies of **8** (Figure 4B) demonstrate strong $^{57}$Fe hyperfine coupling and much slower relaxation properties compared to Fe-$N_2$ **2** (Supporting Information); distinctive features that span a range of 5 mm/s at temperatures of 80 K and lower are observed.

$Fe{=}NNH_2$ **7** is far less stable than **8** and required characterization at cryogenic temperatures. Compound **5′** reacted with $Cp^*_2Co$ in 2-MeTHF at −135 °C to produce dark brown solutions that rapidly bleached when warmed to −78 °C or higher temperatures (*vide infra*). EPR (Figure 4A) and $^{57}$Fe Mössbauer spectra (Figure 4B) collected on similarly prepared frozen reaction mixtures derived from **5′** confirmed the generation of a new $S = {}^1/_2$ species ($g_{avg}$ = 2.04) as the major Fe-containing component. Notably, the $^{57}$Fe Mössbauer spectrum of this complex is nearly identical to that displayed by $Fe{=}NNMe_2$ **8**, allowing us to assign it as the isoelectronic species **7**. Accordingly, the theoretically predicted gas-phase optimized geometry and electronic structure of **7** are very similar to those of **8** (Supporting Information). Compounds **7** and **8** are predicted to have substantial radical character on the $NNR_2$ and phosphine ligands, as also evident from their respective EPR


DOI: 10.1021/jacs.6b01230
J. Am. Chem. Soc. 2016, 138, 4243–4248

**Scheme 3. Comparison of the Reaction Products Observed in the Reduction of (A) Fe=NNH$_2^+$ 5′ and (B) Mo=NNH$_2^+$ Supported by the Tri(amido)amine [HIPTN$_3$N]$^{3-}$ Ligand Framework[19]**

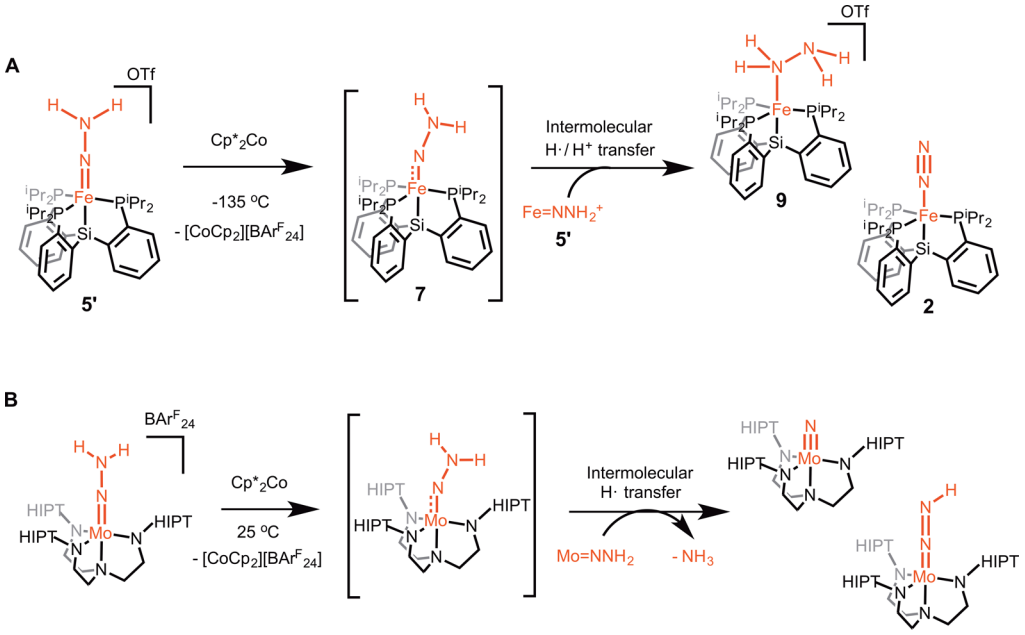


data. Differences between the X-band EPR spectra of $^{15}$N-**8** and **8** establish strong hyperfine coupling (ca. 30 MHz) to a single N-atom (Inset of Figure 4A). In addition, marked differences in the EPR spectra of Fe=NNH$_2$ **7** and Fe=NND$_2$ **7-*d*$_2$** demonstrate significant hyperfine coupling to one or both nitrogen-bound H-atom(s); this value is estimated to be as high as 25 MHz through analysis of the second derivative EPR spectrum at $g_2$ and $g_3$ (Supporting Information). The related $S$ = $^1/_2$ {[TPB]Fe=NNH$_2$}$^+$ exhibited $^1$H hyperfine coupling as large as 18 MHz between $g_2$ and $g_3$.[7]

**Conversion of [SiP$^{iPr}_3$]Fe=NNH$_2^+$ to [SiP$^{iPr}_3$]Fe-NH$_2$NH$_2^+$.** Upon warming to temperatures of −78 °C and higher, solutions that contain Fe=NNH$_2$ **7** and Fe=NNH$_2^+$ **5′** undergo a spontaneous disproportionation to a mixture of Fe species that include the previously reported iron hydrazine complex, {[SiP$^{iPr}_3$]Fe(NH$_2$NH$_2$)}{OTf} (**9**),[9a] as a major component. Thawing THF solutions of **5′** were combined with stoichiometric Cp*$_2$Co and allowed to warm slowly to room temperature over 10 min. After minimal workup, NMR analyses of the resulting mixtures (Supporting Information) revealed the formation of roughly equal amounts of Fe-NH$_2$NH$_2^+$ **9** and Fe-N$_2$ **2** as major products, alongside small amounts of [SiP$^{iPr}_3$]Fe(OTf) (**10**) and {[SiP$^{iPr}_3$]Fe(NH$_3$)}-{OTf} (**11**).[9a] **9** was also detected in a one-pot reaction from Fe-N$_2^-$ **1** via the sequential addition of 2 equiv of HOTf and 0.5 equiv of Cp*$_2$Co to **1** in 2-MeTHF at −135 °C. Significant quantities of free N$_2$H$_4$ (0.53(6) equiv per Fe) and NH$_3$ (0.16(2) equiv) were detected when these reaction mixtures were quenched with HCl 10 min after warming. This product distribution was found to be time dependent: reaction mixtures quenched after standing at room temperature for 24 h revealed the presence of 0.27(6) equiv of N$_2$H$_4$ and 0.39(5) equiv of NH$_3$, establishing further conversion of N$_2$H$_4$ to NH$_3$ in these mixtures.

The overall formation of both N$_2$H$_4$ and NH$_3$ from an Fe=NNH$_2^+$/Fe=NNH$_2$ redox pair is interesting, given that the complex [SiP$^{Ph}_3$]Fe(N$_2$) was previously observed to liberate significant amounts of N$_2$H$_4$ upon exposure to HBF$_4$(Et$_2$O) and CrCl$_2$,[18] whereas the anion {[SiP$^{iPr}_3$]Fe(N$_2$)}$^-$ was instead observed to liberate NH$_3$ in the presence of KC$_8$ and {H(OEt$_2$)$_2$}{BAr$^F_{24}$};[5] N$_2$H$_4$ is anticipated to gradually degrade to NH$_3$ under the latter conditions[5] and hence, even if formed as an intermediate product, its concentration may not build up.

The formation of the Fe-containing products Fe-NH$_2$NH$_2^+$ **9** and Fe-N$_2$ **2** can most simply be rationalized by the reaction sequence shown in Scheme 3. As discussed above, $^{57}$Fe Mössbauer and EPR studies indicate that **5′** is reduced by Cp*$_2$Co to generate neutral Fe=NNH$_2$ **7** at temperatures as low as −135 °C. At higher temperatures, we speculate that *in situ*-generated **7** reacts bimolecularly with remaining **5′** in solution. Exchange of H$^+$ and e$^-$ equivalents between these two compounds results in the formation of neutral Fe-N$_2$ **2** and cationic Fe-NH$_2$NH$_2^+$ **9** as the overall reaction products. Whereas **2** is stable to the presence of Cp*$_2$Co, **9** is slowly reduced by Cp*$_2$Co to afford detectable quantities of NH$_3$ and thereby a mixture of **2** and Fe-OTf **10**. DFT studies predict that the conversion of **5′** + **7** → **2** + **9** is highly exergonic (−45 kcal/mol) (Supporting Information).

## CONCLUSIONS

The present study has described the thorough characterization, including the first crystallographic evidence, of a terminally bonded Fe=NNH$_2$ species via the X-ray structures of **5** and **5′**; these complexes are derived from the activation and protonation of N$_2$ coordinated to iron. Numerous examples of iron oxos, nitrides, and imides featuring strong, covalent iron-to-ligand multiples bonds have been characterized in the past 15 years.[20] The possibility to use such covalency as a strategy for N$_2$ reduction to NH$_3$ is a plausible one, and the stoichiometric chemistry established with the present tris(phosphino)silyl iron system underscores this point. Our ability to isolate diamagnetic [SiP$^{iPr}_3$]Fe=NNH$_2^+$ and its more stable methylated analogue, [SiP$^{iPr}_3$]Fe=NNMe$_2^+$, enables their thorough characterization and also a study of their one-electron reduction chemistry. The stable $S$ = $^1/_2$ complex [SiP$^{iPr}_3$]Fe=NNMe$_2$ has been structurally characterized, and its other spectroscopic parame-



DOI: 10.1021/jacs.6b01230
J. Am. Chem. Soc. 2016, 138, 4243−4248

ters are very similar to those of the far less stable $S = {}^1/_2$ species $[SiP^{iPr}_3]Fe{=}NNH_2$, which must instead be characterized at very low temperature. Each $S = {}^1/_2$ species evidences significant spin-leakage onto the hydrazido ligand.

A fascinating transformation occurs as solutions containing *in situ*-generated $[SiP^{iPr}_3]Fe{=}NNH_2$ and $[SiP^{iPr}_3]Fe{=}NNH_2^+$ are allowed to warm, disproportionating to $[SiP^{iPr}_3]Fe\text{-}NH_2NH_2^+$ and $[SiP^{iPr}_3]Fe\text{-}N_2$. Some $[SiP^{iPr}_3]Fe\text{-}NH_3^+$ is also produced in this process; we had previously shown that $[SiP^{iPr}_3]Fe\text{-}NH_2NH_2^+$ can liberate $[SiP^{iPr}_3]Fe\text{-}NH_3^+$ and free $NH_3$ in solution.[9a] Hence, these collective observations show that iron-bound $N_2$ can be protonated to generate a distal[8] intermediate, $[SiP^{iPr}_3]Fe{=}NNH_2^+$, and further reduced/disproportionated to an alternating intermediate,[8] $[SiP^{iPr}_3]Fe\text{-}NH_2NH_2^+$, that serves as a source of $NH_3$ via late-stage N−N cleavage. The conversion of $N_2$ to $NH_3$ via an $N_2H_4$ intermediate therefore does not require an alternating pathway; it can instead be initiated along a distal pathway. Such a scenario is distinct from the early stage N−N cleavage pathway to generate terminal nitrides that is thought to occur in the molybdenum $N_2$ reduction catalysts of Schrock and Nishibayashi, respectively.[4]

The catalytically relevant $[TPB]Fe\text{-}N_2^-$ system is thought to proceed via a distal $S = {}^1/_2$ $[TPB]Fe{=}NNH_2^+$ intermediate.[7] This species cannot be isolated owing to its greater instability and the presence of additional iron components, and it remains unclear whether $NH_3$ production in this case derives from similar late-stage cleavage to first produce $N_2H_4$, akin to $[SiP^{iPr}_3]Fe{=}NNH_2$, or if an early-stage cleavage pathway instead generates a terminal iron-bound nitride, such as $[TPB]Fe{\equiv}N$ or $(TPB)Fe{\equiv}N^+$. The greater flexibility of the Fe−B bond relative to the Fe−Si bond may afford access to different intermediates. However, that $[SiP^{iPr}_3]Fe\text{-}N_2^-$ generates appreciable amounts of $NH_3$ under the same conditions as $[TPB]Fe\text{-}N_2^-$, and that its isostructural carbon analogue $[CP^{iPr}_3]Fe\text{-}N_2^-$ is a catalyst for $N_2$-to-$NH_3$ conversion but is not as flexible as the $[TPB]Fe$ system,[5b] suggests the possibility and perhaps likelihood of a unifying distal-to-alternating mechanistic sequence en route to $NH_3$ for these three iron systems.

While we have here demonstrated the viability of a hybrid distal-to-alternating reaction pathway for $NH_3$ generation via $N_2H_4$, we still caution that different Fe-mediated $N_2$ reduction systems, with variable reaction conditions, may sample alternative pathways.

## ■ ASSOCIATED CONTENT

### Supporting Information

The Supporting Information is available free of charge on the ACS Publications website at DOI: 10.1021/jacs.6b01230.

Detailed experimental, spectroscopic, and theoretical data (PDF)

X-ray crystallographic data for **1**, **5**, **5′**, **6**, and **8** (CIF)

## ■ AUTHOR INFORMATION


### Corresponding Author

*jpeters@caltech.edu


### Notes

The authors declare no competing financial interest.

## ■ ACKNOWLEDGMENTS

This work was supported by the NIH (GM 070757) and the Gordon and Betty Moore Foundation. J.R. was additionally supported by a fellowship from the Caltech Center for Environmental Microbial Interactions (CEMI).

## ■ REFERENCES


(1) Howard, J. B.; Rees, D. C. *Chem. Rev.* **1996**, *96*, 2965−2982.

(2) (a) Lancaster, K. M.; Roemelt, M.; Ettenhuber, P.; Hu, Y.; Ribbe, M. W.; Neese, F.; Bergmann, U.; DeBeer, S. *Science* **2011**, *334*, 974−977. (b) Seefeldt, L. C.; Hoffman, B. M.; Dean, D. R. *Annu. Rev. Biochem.* **2009**, *78*, 701−722. (c) Spatzal, T.; Perez, K. A.; Einsle, O.; Howard, J. B.; Rees, D. C. *Science* **2014**, *345*, 1620−1623. (d) Hinnemann, B.; Norskov, J. K. *Top. Catal.* **2006**, *37*, 55−70.

(3) (a) Schrock, R. R. *Acc. Chem. Res.* **2005**, *38*, 955−962. (b) Nishibayashi, Y. *Inorg. Chem.* **2015**, *54*, 9234−9247. (c) McWilliams, S. F.; Holland, P. L. *Acc. Chem. Res.* **2015**, *48*, 2059−2065.

(4) (a) Yandulov, D. V.; Schrock, R. R. *Science* **2003**, *301*, 76−78. (b) Arashiba, K.; Kinoshita, E.; Kuriyama, S.; Eizawa, A.; Nakajima, K.; Tanaka, H.; Yoshizawa, K.; Nishibayashi, Y. *J. Am. Chem. Soc.* **2015**, *137*, 5666−5669. (c) Arashiba, K.; Miyake, Y.; Nishibayashi, Y. *Nat. Chem.* **2011**, *3*, 120−125.

(5) (a) Anderson, J. S.; Rittle, J.; Peters, J. C. *Nature* **2013**, *501*, 84−87. (b) Creutz, S. E.; Peters, J. C. *J. Am. Chem. Soc.* **2014**, *136*, 1105−1115. (c) Ung, G.; Peters, J. C. *Angew. Chem., Int. Ed.* **2015**, *54*, 532−535.

(6) (a) Chatt, J.; Dilworth, J. R.; Richards, R. L. *Chem. Rev.* **1978**, *78*, 589−625. (b) Yandulov, D. V.; Schrock, R. R. *J. Am. Chem. Soc.* **2002**, *124*, 6252−6253. (c) Hidai, M.; Mizobe, Y. *Chem. Rev.* **1995**, *95*, 1115−1133.

(7) Anderson, J. S.; Cutsail, G. E.; Rittle, J.; Connor, B. A.; Gunderson, W. A.; Zhang, L.; Hoffman, B. M.; Peters, J. C. *J. Am. Chem. Soc.* **2015**, *137*, 7803−7809.

(8) Hoffman, B. M.; Lukoyanov, D.; Dean, D. R.; Seefeldt, L. C. *Acc. Chem. Res.* **2013**, *46*, 587−595.

(9) (a) Lee, Y.; Mankad, N. P.; Peters, J. C. *Nat. Chem.* **2010**, *2*, 558−565. (b) Mankad, N. P.; Muller, P.; Peters, J. C. *J. Am. Chem. Soc.* **2010**, *132*, 4083−4085. (c) Lee, Y.; Peters, J. C. *J. Am. Chem. Soc.* **2011**, *133*, 4438−4446.

(10) Fong, H.; Moret, M.-E.; Lee, Y.; Peters, J. C. *Organometallics* **2013**, *32*, 3053−3062.

(11) Lehnert, N.; Tuczek, F. *Inorg. Chem.* **1999**, *38*, 1659−1670.

(12) Steiner, T. *Angew. Chem., Int. Ed.* **2002**, *41*, 48−76.

(13) Field, L. D.; Li, H. L.; Dalgarno, S. J.; Turner, P. *Chem. Commun.* **2008**, 1680−1682.

(14) (a) Sellmann, D.; Soglowek, W.; Knoch, F.; Moll, M. *Angew. Chem., Int. Ed. Engl.* **1989**, *28*, 1271−1272. (b) Saouma, C. T.; Muller, P.; Peters, J. C. *J. Am. Chem. Soc.* **2009**, *131*, 10358−10359. (c) Li, Y.; Li, Y.; Wang, B.; Luo, Y.; Yang, D.; Tong, P.; Zhao, J.; Luo, L.; Zhou, Y.; Chen, S.; Cheng, F.; Qu, J. *Nat. Chem.* **2013**, *5*, 320−326.

(15) Solutions of **6** display temperature-dependent paramagnetism consistent with a low-lying triplet state (see Supporting Information for additional details).

(16) Donovan-Mtunzi, S.; Richards, R. L.; Mason, J. *J. Chem. Soc., Dalton Trans.* **1984**, 1329−1332.

(17) Binsch, G.; Lambert, J. B.; Roberts, B. W.; Roberts, J. D. *J. Am. Chem. Soc.* **1964**, *86*, 5564−5570.

(18) Mankad, N. P.; Whited, M. T.; Peters, J. C. *Angew. Chem., Int. Ed.* **2007**, *46*, 5768−5771.

(19) (a) Yandulov, D. V.; Schrock, R. R. *Inorg. Chem.* **2005**, *44*, 1103−1117. (b) Schrock, R. R. *Angew. Chem., Int. Ed.* **2008**, *47*, 5512−5522. (c) Schenk, S.; Le Guennic, B.; Kirchner, B.; Reiher, M. *Inorg. Chem.* **2008**, *47*, 3634−3650.

(20) (a) Saouma, C. T.; Peters, J. C. *Coord. Chem. Rev.* **2011**, *255*, 920−937. (b) Hohenberger, J.; Ray, K.; Meyer, K. *Nat. Commun.* **2012**, *3*, 720.




DOI: 10.1021/jacs.6b01230
*J. Am. Chem. Soc.* 2016, 138, 4243−4248